Astron. Astrophys. 326, 465–476 (1997)

ASTRONOMY AND ASTROPHYSICS

# Observational signatures of helical galactic magnetic fields

**M. Urbanik**[1], **D. Elstner**[2], **and R. Beck**[3]

[1] Astronomical Observatory, Jagiellonian University, Krakow, Poland
[2] Astrophysikalisches Institut Potsdam, An der Sternwarte 16, D-14482 Potsdam, Germany
[3] Max-Planck-Institut für Radioastronomie, Postfach 2024, D-53010 Bonn, Germany

Received 28 February 1997 / Accepted 23 May 1997

**Abstract.** We investigate the possibility of reproducing the observed polarization and Faraday rotation properties of spiral galaxies assuming their disks to be filled with regular helical magnetic fields. Both small-scale ($< 1$ kpc) flux tubes predicted by local hydrodynamic models and global, galaxy-scale (several kpc) fields generated by the dynamo process are considered. The large-scale fields are found to well reproduce the observed regular spiral pattern of polarization B vectors, as well as asymmetries of Faraday rotation and low-frequency polarization, often believed to signify non-axisymmetric or bisymmetric fields.

**Key words:** galaxies: magnetic fields – galaxies: spiral – radio continuum: galaxies – polarization – galaxies: individual: NGC 6946 – MHD

## 1. Introduction

As shown by numerical simulations (Otmianowska-Mazur et al. 1992, Otmianowska-Mazur & Urbanik 1994) interstellar turbulence and magnetic diffusion leads to the growth of radial and vertical magnetic field components which together with the azimuthal field form tubes twisted helically over scales of several hundreds of parsecs. Their growth may become limited by the stress of magnetic lines, leading to a galactic disk filled with a large number of individual tubes. Alternatively, their size can increase continuously, giving rise to galaxy-scale vertical, radial and azimuthal fields. The first two of them together give the poloidal magnetic field, forming loops in the plane perpendicular to the local azimuthal direction. A combination of toroidal and poloidal fields, yields three-dimensional, helical structures of magnetic lines on a galactic scale (see Donner & Brandenburg 1990). The formation of such structures is well described by the mean-field equations in the framework of the dynamo theory (Wielebinski & Krause 1993). In differentially rotating, flat galactic disks the axisymmetric quadrupole (S0) mode is the easiest one to amplify by dynamo action (cf. Elstner et al. 1992). The discrimination between the generation of small-scale tubes or galaxy-scale fields on theoretical grounds alone would require complex non-linear calculations. The current magnetic field theories do not yet set any definite limits to the scale of field twisting, leaving it open to observational estimates.

The preponderance of axisymmetric helical fields in galactic disks is sometimes questioned on both theoretical and observational grounds. In particular, theories assuming field amplification by spiral arms (Chiba 1993, Lesch 1993) yield amplification of non-axisymmetric structures.

Though Soida et al. (1996) present clear evidence in support of the existence of axisymmetric magnetic fields even in a highly perturbed galaxy, some polarization studies of nearby spirals are suggestive for strongly asymmetric field structures. In particular, observations at low frequencies (subject to significant Faraday rotation and depolarization) show the polarized emission forming crescent-like structures asymmetrically encircling the outer disk or depolarized channels on one disk side (Sukumar & Allen 1989, Beck 1991, Neininger et al. 1993). The variations of Faraday rotation with the azimuthal angle in the disk are sometimes used as arguments for non-axisymmetric fields, as well. In particular, the doubly-periodic variation of the rotation measure ($RM$) in the highly inclined galaxy M81 (Krause et al. 1989) is considered as evidence for bisymmetric (BSS) magnetic fields though this object is the only convincing example of the effect (Beck et al. 1996).

The main difficulty in straightforward interpretations of the polarization data is the fact that the magnetic fields possess complex three-dimensional structures with a large-scale vertical component causing strong Faraday effects even in nearly face-on spirals. The polarized intensity (especially at low frequencies) seen by the radio telescope contains contributions from parts of the field structure at different depths along the line of sight, integrated over the whole pathlength through the galaxy and over the telescope beamwidth. The received signal is additionally modified by Faraday effects varying along the line of sight and within the beam. The observed polarization of the galaxy (including the signatures of non-axisymmetric fields) is thus a result of a complex interplay of effects of projection and limited resolution.

*Send offprint requests to*: M. Urbanik

The observational properties of particular magnetic field structures can be studied using polarization and Faraday rotation modeling techniques. As helical magnetic fields constitute the natural outcome of interstellar gas kinematics and the dynamo process (Otmianowska-Mazur & Urbanik 1994, Pouquet et al. 1976) and their existence seems to be supported by high-frequency observations of perturbed galaxies (Soida et al. 1996), we use beam-smoothed models to study the observational signatures of such field configurations in more detail. In particular we try to answer the question to which extent the polarization and Faraday rotation properties of nearby galaxies can be explained in the framework of axisymmetric, helical field models possessing various scales.

In the present work we construct the distributions of polarized intensity and polarization B vectors as emitted by a model galactic disk filled with axisymmetric magnetic field structures. Effects of Faraday rotation and depolarization are included, as well. Our results are compared to available radio polarization data for nearby galaxies.

## 2. Model description

### 2.1. General assumptions

In our models we considered magnetic fields twisted over scales of several hundreds of parsecs (called here small-scale fields) and those predicted by mean-field dynamo theory. The galactic disks were also assumed to contain cosmic-ray (CR) electrons and thermal gas with densities $N_e$ and $N_{th}$, respectively, varying with altitude above the disk as Gaussian functions. Their vertical scale heights were independent and adjustable model parameters. At the present stage of the model $N_e$ and $N_{th}$ did not depend on the galactocentric radius. Our calculations did not involve any random fields which are responsible for a large fraction of the total field energy, thus our models did not need any assumptions concerning equipartition or pressure balance between the total magnetic and CR energy densities. This allowed us to set independently $N_e$, $N_{th}$, their vertical scale heights, as well as the distribution of the uniform field strength. As no random fields were considered, no account for opacity effects due to Faraday dispersion was made at this model stage.

In our computations we assumed that the galactic radio emission is purely synchrotron, with a straight spectrum and a spectral index $\alpha$ = 0.8 ($I_\nu \propto \nu^{-\alpha}$). As we were not interested in absolute values of the total power and polarized brightness but in their distributions over the disk only, the magnetic field and the CR electron density units were arbitrary, and the model was normalized in such a way that the peak of the total power brightness was always 10000. This made it independent of assumptions concerning mean magnetic field strengths and cosmic-ray electron densities in physical units. To keep our model free of assumptions concerning the magnetic field strengths also in computing the Faraday rotation, we normalized it using the angle of rotation of the polarization plane in a unit magnetic field parallel to the line of sight over a unit pathlength. This made the assumed observational frequencies unitless as well. However, we could define a "Faraday-thick" or low-frequency domain in which the Faraday rotation angle $\Delta\chi$ along the average pathlength through the disk approaches or exceeds $90^o$. In face-on galaxies with typical ionized gas densities this corresponds roughly to $\nu \leq 1.4$ GHz. Conversely, we defined a "Faraday-thin" or high-frequency range with maximum $\Delta\chi << 90^o$. In typical face-on galaxies this is the case for $\nu \geq 5$ GHz, though if the ionized gas content is very low the "Faraday-thin" domain may extend down to much lower frequencies.

### 2.2. Magnetic field structures

At the present stage of modeling we made a first-order approximation of the magnetic field structure by adopting axisymmetric magnetic fields without accounting for possible azimuthal variations of the uniform field strength related to e.g. magnetic spiral arms (Beck & Hoernes 1996). The azimuthal modulation of the polarized intensity is evident only in high resolution observations, being much weaker for the beam of 2 kpc used in our models. Thus, neglecting the azimuthal modulation should not change significantly our results.

In case of small-scale fields we analyzed helically twisted magnetic tubes with lines of force wrapped around the tube axis at a constant, adopted twist angle (Fig. 1a). Above and below the galactic plane the field twist was adopted to be of opposite sense (Fig. 1b), in agreement with the concept of helical field generation by Coriolis force-driven turbulence (Otmianowska-Mazur & Urbanik 1994). The azimuthal field filled the tubes uniformly and had the same direction in the whole disk. The galaxy was assumed to contain a number of tightly packed tubes, parallel to the plane and running concentrically in the azimuthal direction around the disk (Fig. 1b). The tube size and the field twist angle inside the tubes were free parameters.

In the case of global, galaxy-scale fields we used two kinds of structures:

a.) Analytical approximations of the simplest, axisymmetric dynamo fields, resembling those computed by Elstner et al. (1992). The adopted magnetic field consisted of an adjustable mixture of two basic components (see Fig. 2): the poloidal S0 field with assumed vertical and radial component distributions, and a toroidal field of an assumed strength relative to the poloidal one, also with an adjustable vertical scale height and radial distribution. No radial reversals of the toroidal component were considered. To satisfy the condition div $B = 0$, the poloidal field components were computed by adopting an appropriate shape of the potential $A(r, z)$, followed by computing the magnetic field components $B_r$ and $B_z$ as:

$$B_r = -(\partial A/\partial z), \qquad (1)$$

$$B_z = 1/r(\partial r A/\partial r), \qquad (2)$$

where r and z are the galactocentric radius and height above the disk, respectively. Using the analytical approximation this allowed us to quickly vary the magnetic field geometry without extremely time-consuming dynamo calculations. In

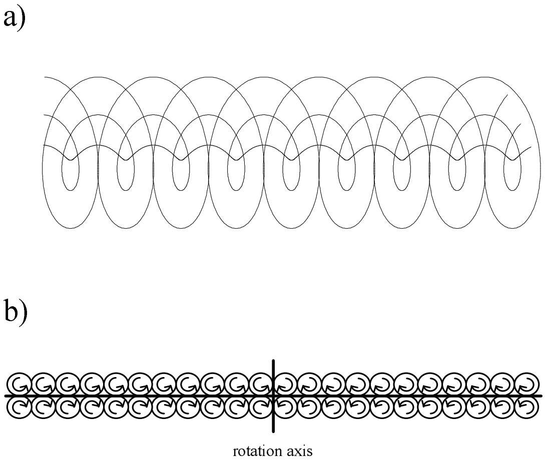


**Fig. 1a and b.** Small-scale fields used in models of the polarized intensity of galactic disks. A perspective view of selected magnetic lines in a single tube (**a**) and a vertical cross-section of the galactic disk viewed edge-on, filled with concentrically arranged small-scale tubes (**b**). A horizontal line marks the galactic plane. Arrows inside tubes mark the directions of twist of the poloidal component in each tube. The toroidal field is unidirectional and fills the tube interiors uniformly

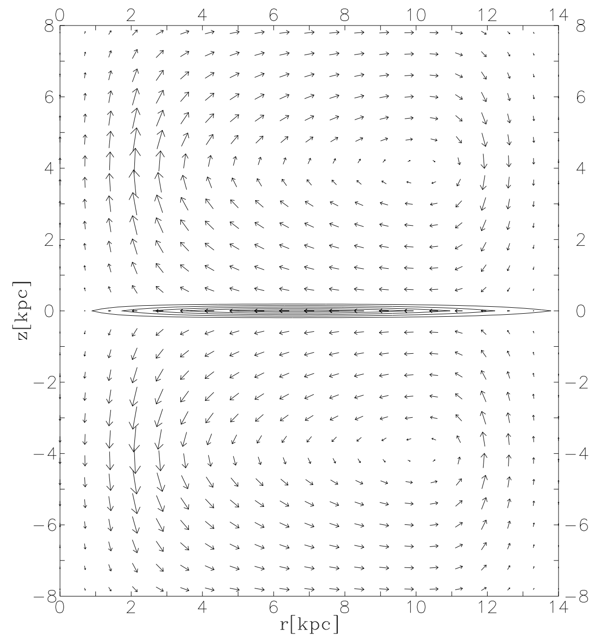


**Fig. 2.** An example of an analytically approximated axisymmetric field with an extended magnetic halo (see text) used for models of polarized emission from large-scale magnetic fields. The figure shows a vertical cross-section of one half of the galactic disk; the rotation axis is on the left-hand side of the picture. Arrows represent vectors of the poloidal component while contours show isolines of the toroidal field strength

particular, we could look for magnetic field structures providing the best reproduction of observations even when the required particular field configuration has not yet been obtained strictly from the dynamo theory in its present state. This allowed us to define requirements for the dynamo models, necessary to explain specific observational facts. During the computations we assumed either an extended magnetic halo shown in Fig. 2 with a vertical extent of the poloidal field of 8 kpc, or a magnetic disk with a poloidal field of similar topology, but looping within 2 kpc from the plane, with a turning point of $B_r$ at a height of 1 kpc. To attain the best agreement with observations we adjusted the details of radial and vertical distributions of $B_r$ and $B_z$, as well as the scale height of the toroidal component and its strength relative to the poloidal one.

b) Magnetic fields directly obtained from the linear mean-field dynamo equations (Elstner et al. 1992). To check finally to what extent the existing dynamo results can reproduce the observations, we used an extensive library of dynamo magnetic fields computed at the Astrophysical Institute in Potsdam by one of us (DE). A typical property of these fields is the highly correlated variation of azimuthal and radial field components resulting from an assumed strong differential rotation not only in the disk but also at large heights in the halo, which leads to only mild variations of the intrinsic field pitch angle with r and z. The models with strong poloidal fields also possess quite a strong, toroidal field in the halo, reversing its direction about 2-3 kpc above the disk plane (as postulated for M51 by Berkhuijsen et al. 1996). The confrontation of the results for such fields with those for the analytical approximations as well as the use of some algebraic modifications of the dynamo-computed fields (e.g. changing the ratio of the poloidal to toroidal component) allowed us to put some constraints on the magnetic fields computed from dynamo models.

### *2.3. Methods of modeling*

For small scales the disk was adopted to be filled with a number of magnetic tubes running around the disk (Fig. 1). Each tube was divided into 80 azimuthal slices, corresponding to the interval of azimuthal angle in the disk of $4.5^o$. Each slice was divided internally into 15 radial and 13 angular elements. For large-scale fields the disk was divided into 80 azimuthal sectors, each consisting of up to 60 radial slices and 80 slices along the vertical coordinate, depending on the field model. The same method was used for analytical fields as well as for those computed from the dynamo equations.

The disk was inclined to the sky plane by an adopted angle. All calculations were made in coordinates x and y parallel to the sky and in particular, to major and minor axes of the projected disk, respectively. For both types of the field structure we computed for each element its contribution to Stokes parameters $I$, $Q$ and $U$.

$$I = FN_e(z)B_\perp^{1+\alpha}\Delta V, \quad (3)$$

$$Q = 0.73I\cos\chi, \quad (4)$$

$$U = 0.73I\sin\chi, \quad (5)$$

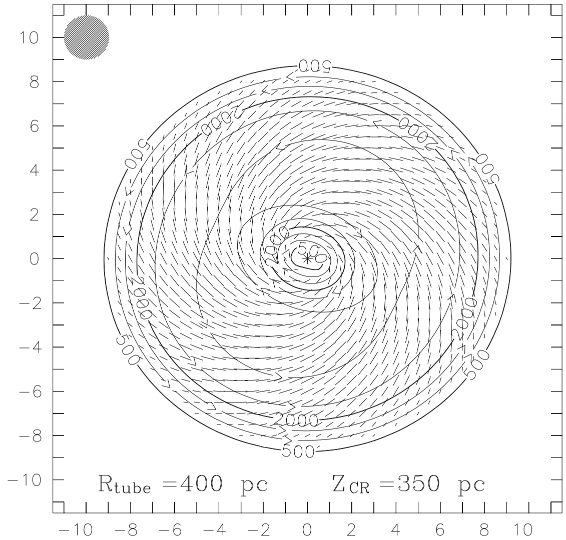


**Fig. 3.** The contours of polarized intensity and the distribution of polarization B vectors for the model of a disk filled with small-scale tubes 400 pc in radius. A vertical CR scale height of 350 pc is assumed. The galaxy's inclination is $30^o$

where $B_\perp = (B_x^2 + B_y^2)^{1/2}$ is the locally computed uniform magnetic field component perpendicular to the line of sight, $B_x$ and $B_y$ are the components of $B_\perp$ parallel to major and minor axes of the projected disk, respectively, $N_e$(z) is the cosmic-ray electron density at the height z relative to that in the disk plane, $F$ is the normalization constant adjusted to yield the peak total power brightness of 10000, $\alpha$ is the assumed spectral index, $\Delta V$ is the element volume and 0.73 is the maximum polarization degree in a perfectly uniform magnetic field for a spectral index of 0.8 (Pacholczyk 1970). The position angles of electric vectors in our x-y frame were computed by integrating the Faraday rotation along the line of sight:

$$\chi = \arctan(B_y/B_x) + C \int_0^s B_\parallel(s) N_{th}(z) ds \qquad (6)$$

where $B_\parallel$ is the magnetic field component parallel to the line of sight, $N_{th}$ is the density of thermal electrons relative to that in the disk plane, and $C$ is the Faraday rotation per unit pathlength, unit $B_\parallel$ and unit $N_{th}$.

The beam-smoothed contributions from all the elements yielded the model maps of the Stokes parameters considered, from which distributions of total power, polarized intensity and polarization angle were obtained. All were rotated, if necessary, to the galaxy's position angle on the sky. A comparison of maps computed at two frequencies (i.e. with different values of the constant $C$ in Eq. 6) also yielded distributions of rotation measure. The variations of this quantity with azimuthal angle in the disk, integrated in sectors of $15^o$ width, were obtained as well.

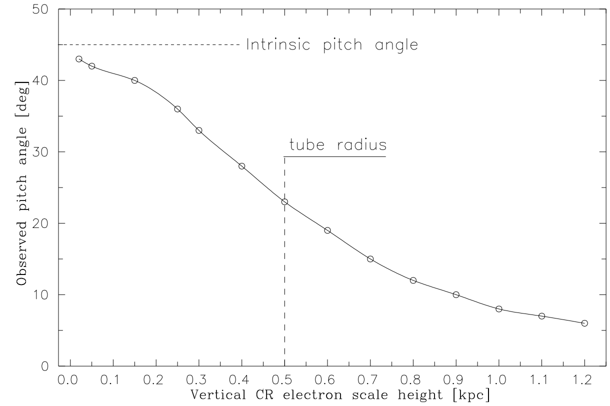


**Fig. 4.** Changes of the observed pitch angle of the B vectors with vertical scale height of CR electrons for the model with tubes 500 pc in radius and an intrinsic angle of the field twist of $45^o$

## 3. Results

### 3.1. High-frequency distributions of the polarized intensity

At high frequencies (small Faraday rotation) both small- and large-scale fields yield a similar coherent spiral-like arrangement of B vectors of the polarized emission. We will call it hereinafter "a spiral pattern of B vectors", though no distinct spiral arm were obtained. For dynamo-type fields this pattern has been demonstrated and discussed in detail by Elstner et al (1992). Fig. 3 shows the coherent spiral pattern of B vectors for the disk filled with 11 tubes having a radius of 400 pc and a field twist angle inside the tubes of $45^o$. A global spiral pattern of the observed B vectors can in principle be obtained with magnetic fields twisted over spatial scales of only a few hundred parsecs, thus a coherent spiral structure of B vectors alone does not provide direct evidence for the existence of global-scale poloidal magnetic fields.

In case of small magnetic tubes (Fig. 1) and a CR-electron disk thinner than their diameter only the magnetic line segments closest to the disk plane are visible in synchrotron radiation. Both above and below the disk plane they possess a radial component directed always towards the galaxy center, added to an azimuthal field $B_\phi$. A face-on view would show these magnetic line segments, distributed along the places where the tubes touch the plane and inclined everywhere to the azimuthal direction by the same pitch angle $\psi$=arctan($B_r/B_\phi$). Their beam-smeared contributions give rise to a pattern of B vectors systematically inclined to the azimuthal direction, as shown in Fig. 3. The tube halves more distant from the disk yield an opposite sign of $\psi$ because of a reversed sign of $B_r$ (see Fig. 1). With an increasing CR electron scale height, their growing contribution leads to a decrease of mean $B_r$ integrated over the line of sight, thus to a decrease of an observed pitch angle of polarization B vectors.

Fig. 3 was obtained for quite a small cosmic-ray electron scale height of 350 pc. This is considerably smaller than the synchrotron disk scale height of 1 kpc in edge-on spirals (see

Tab. 1 in Beck 1997), implying an even greater scale height for CR electrons if the total field strength decreases also with distance from the disk plane. If we increase the CR scale height to realistic values, the pitch angle of the B vectors for tubes having less than 1 kpc in diameter becomes very small (Fig. 4). If we want to obtain the polarization pattern shown in Fig. 3 with the pitch angle of B vectors of 20-30$^o$ and for the CR-electron scale height of 1 kpc, tubes having poloidal and toroidal fields of similar strengths would have radii of order of 2 kpc, thus diameters of 4 kpc, comparable to scales of large-scale fields. Smaller tubes would require a poloidal field much stronger than the toroidal one, which in edge-on objects would produce a picture dominated by vertical fields. As such effects are not observed, all this constitutes the main difficulty of small-scale models.

For all kinds of the magnetic field geometry only the part of the field structure having the distance from the galactic plane smaller or equal to the CR-electron scale height is seen in emission. A combination of radial and toroidal fields in this region well reproduces the regular spiral pattern of observed B vectors without strong constraints upon the vertical CR scale (see Elstner et al. 1992). For the magnetic field shown in Fig. 2 an increase of the CR-electron scale height would make the observed pitch angle observed in a face-on disk even larger, because of $B_\phi$ decreasing quickly with z. The dynamo-computed fields from our collection exhibit little spatial changes of the intrinsic field pitch angle because of quite a strong, reversed toroidal field in the halo (see Sect. 2.2). This makes their observed picture rather insensitive to changes of the CR-electron scale height. We also note that for the CR-electron scale height of 1 kpc the edge-on view of the magnetic field shown in Fig. 2 would show mostly B vectors parallel to the disk and little evidence for strong vertical fields. As all the above makes the large-scale fields more promising in explaining the observed polarization structure of spiral galaxies, small-scale tubes were not considered further.

In our models the pitch angle $\psi$ of polarization B vectors is found to vary periodically with the azimuthal angle in the disk, in agreement with observations (e.g. NGC 6946, Ehle & Beck 1993). For our dynamo fields, showing mild variations of the intrinsic pitch angle of the field with r and z, the effect is generally weak and has an amplitude of the order of 1$^o$. In Fig. 5 we show the azimuthal variations of $\psi$ for the dynamo field yielding the highest amplitude of this effect among the dynamo models from our collection. A much higher amplitude of about 8$^o$ is found for our analytical field shown in Fig. 2, in which independently varying azimuthal and radial components lead to strong intrinsic pitch angle changes with r and z. However, when the galactic disk is filled with the same poloidal field as in Fig. 2 and the azimuthal component is proportional everywhere to the radial one (yielding a constant intrinsic pitch angle), the effect disappears in erratic fluctuations due to projection and beam-smearing effects. Thus, the observed azimuthal variations of $\psi$ may be due to changes of the ratio of azimuthal to radial components with radius and distance from the plane and do not necessarily imply deviations from the field axial symmetry.

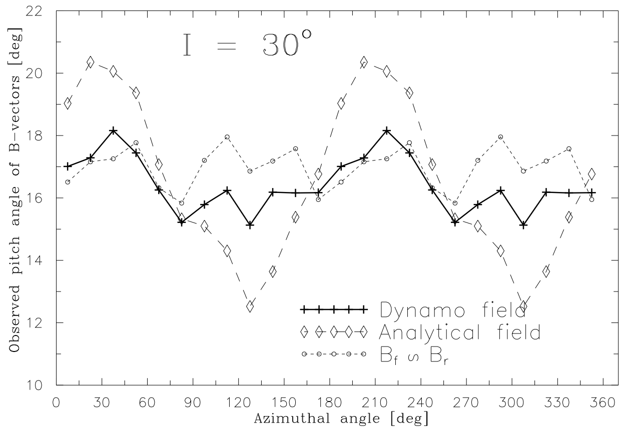


**Fig. 5.** Variations of pitch angle of B vectors (corrected to face-on position) with azimuthal angle in the disk for three models of axisymmetric fields: a dynamo-computed field possessing the largest intrinsic pitch angle among our dynamo fields (thick line), our analytical model shown in Fig. 2 with the azimuthal component adjusted to give a mean pitch angle similar to that of the dynamo field discussed (dashed line), and the analytical model with the same poloidal component as in Fig. 2 but the azimuthal field proportional everywhere to the radial one, yielding a constant intrinsic field pitch angle (dotted line)

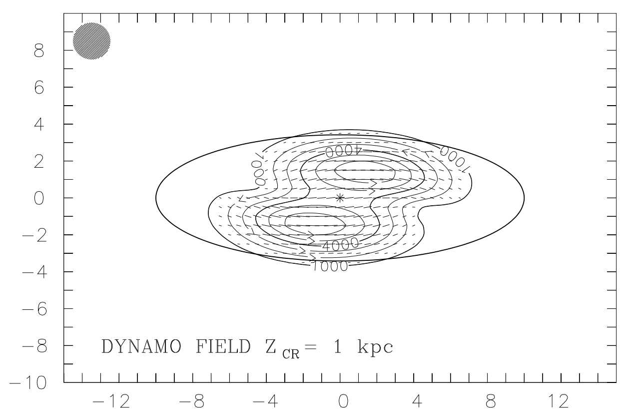


**Fig. 6.** The asymmetry of the distribution of high-frequency polarized intensity of a galactic disk inclined by 70 deg and filled with an axisymmetric dynamo field. The CR electrons were assumed to be contained within a disk of 10 kpc in radius (delineated by the ellipse) and to have a vertical scale height of 1 kpc

A shift of the maxima of polarized intensity in opposite directions away from the minor axis, discussed by Urbanik & Otmianowska-Mazur (1993) for a M31-type galaxy (dominated by a single torus of emission), is also found for disks filled with many small tubes or large-scale axisymmetric fields (Fig. 6, see also Donner & Brandenburg 1990). Its direction depends on the galaxy's orientation in space (i.e. which side is the near one) and on the sign of the azimuthal magnetic field. The effect increases with the inclination of the galaxy, being strongest for an inclination of about 70$^o$, then drops quickly to zero for edge-on objects (see Urbanik & Otmianowska-Mazur 1993). The best

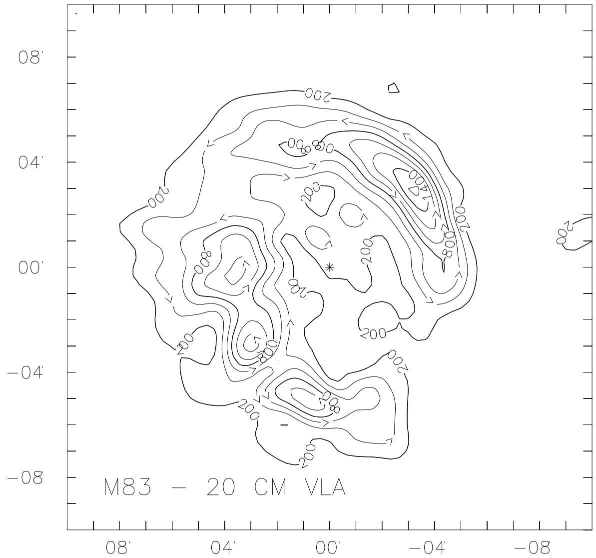


**Fig. 7.** The contour map of the polarized intensity of M83 at 1.49 GHz made from the data of Sukumar and Allen (1989). The scale shows the distance from the map centre in arcmin

observational example of this asymmetry was found in M31 by Beck (1982). Urbanik et al. (1994) succeeded in explaining it on the basis of small-scale helicity of the magnetic field. However, the size of the radio-emitting torus in M31 limits the maximum scale of field twisting to about 1 kpc.

The discussed asymmetry decreases (as do the observed pitch angles) when the CR electron scale height approaches the tube size. This constraint is again relaxed if large-scale fields are considered. A characteristic shift of the maxima of polarized emission on both sides of the minor axis was observed in NGC 7331 by Dumke et al. (1995). Using the analytically approximated dynamo-type S0 fields we could qualitatively reproduce this effect and in particular the asymmetry direction in agreement with the galaxy's spatial orientation and the mean field direction.

Small-scale fields, especially when twisted over scales smaller than the beam size, cause significant geometrical depolarization. In this respect they may at least partly play the role of random fields, lowering the polarization degree (Segalovitz et al. 1976) to observed values. Large-scale fields even when convolved to a beam of 2 kpc, yield a mean polarization degree of order of 50-60%. While quite high polarization is revealed locally by high-resolution studies (e.g. Beck & Hoernes 1996) the mean polarization degree observed with a moderate resolution is lower by a factor of about 3-5. This requires random fields or helical fields twisted on scales $<<$ 1 kpc with a mean strength about 1.5 -2 times that of the large scale-field as an additional ingredient.

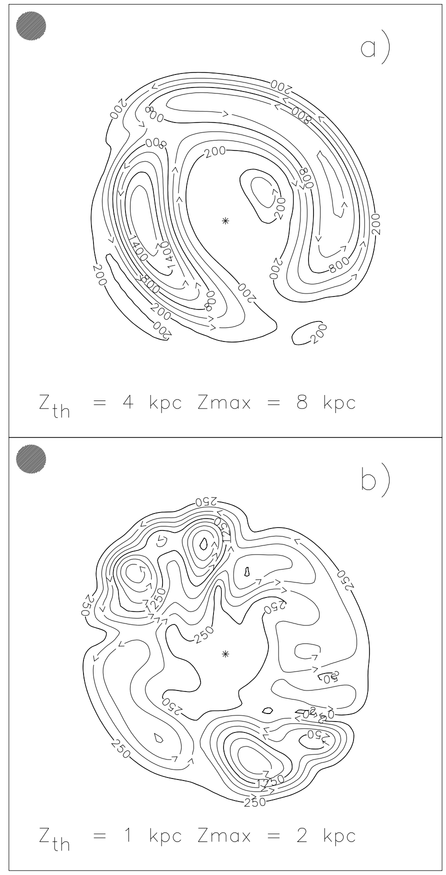


**Fig. 8a and b.** The model of low-frequency polarized emission from M83 for the analytical magnetic fields: **a** for the field shown in Fig. 2 with a poloidal component extending up to 8 kpc from the plane, a toroidal field with a vertical scale height of 100 pc, and a dilute thermal gas with a vertical scale height of 4 kpc, and **b** for the magnetic disk extending only to 2 kpc from the plane and vertical scale height of the thermal gas of 1 kpc. A CR-electron disk with a radius of 10 kpc and a vertical scale height of 1 kpc was adopted. The model has the same inclination and is rotated to the same major axis position angle as M83

### *3.2. The effects of Faraday depolarization*

At low frequencies where Faraday rotation and depolarization effects become important, the polarized intensity in nearby galaxies forms asymmetric arcs encircling the outer disk and leaving a depolarized channel close to one of the major axis ends (Sukumar & Allen 1989, Neininger et al. 1993, see Fig. 7). We found that our model with the thick magnetic halo shown in Fig. 2 can be adjusted to reproduce qualitatively the morphology of the polarized emission of M83 shown in Fig. 7, though details still differ, mainly because of the simplicity of our models (Fig. 8a). By changing details of the distributions of particular components we could attain more resemblance to either M83 or NGC 6946 which was observed at 20 cm by Beck (1991). The best similarity to observed polarization patterns is obtained for a poloidal field penetrating up to 8 kpc into the halo and showing slow variations of the radial field strength with z, while the toroidal field is confined to the immediate vicinity of the disk plane and has a strength similar to the radial one. An extended (Gaussian scale height of 4 kpc) halo of a hot dilute thermal gas was also necessary, in agreement with X-ray observations (Ehle et al. 1997a). Models with magnetic disks of only 2 kpc thickness, assuming a gas scale height of 1 kpc, are found to yield invariably strong polarization maxima close to the major axis ends (Fig. 8b), in strong disagreement with observations, and are generally unable to reproduce the low-frequency polarized rings.

Computations of the whole grid of models in a "Faraday-thick" regime showed that various degrees of low-frequency asymmetry of the polarized brightness distribution occur nearly for all magnetic field models with a strong poloidal component penetrating high into the halo and a large envelope of thermal gas. For a given amount of Faraday rotation per unit pathlength the effect tends to be stronger for a higher ratio of poloidal-to-toroidal fields, though the polarization pattern changes in a complex way with details of the magnetic field geometry. In particular some models with strong Faraday rotation yield quite complex low-frequency polarization structures with multiple maxima and strongly depolarized regions, accompanied by strong jumps of Faraday rotation. A similar kind of morphology is seen in M51 (Horellou et al. 1992) though our present simple models were unable to reproduce more than an overall resemblance.

None of the investigated dynamo fields clearly gave the picture shown in Fig. 7. However, one of the dynamo models with weak turbulent diffusion in the halo, and a poloidal field extending up to 6 kpc above the disk showed some hints of arc-like asymmetry when the original toroidal field strength was reduced by a factor of three. The asymmetry (Fig. 9a) is especially visible when a smooth, symmetric disk emission is subtracted (Fig. 9b). The model thus yields an arc-like structure overlaid on a much brighter symmetric disk of polarized emission (not seen in M83 or NGC 6946). This is possibly due to a thick layer of toroidal field accompanying strong poloidal fields in dynamo models with a differentially rotating halo. A possibility that in real galaxies opacity effects due to Faraday dispersion may suppress the smooth emission, enhancing the contrast of the ring cannot be ruled-out. However, a detailed statement requires a more advanced model involving random fields and dispersion effects. A better agreement with observations can be also attained if the dynamo theory were able to obtain the toroidal component of the magnetic field with considerably reduced strength and vertical extent.

In edge-on galaxies, our models predict one side of the disk to be strongly depolarized. In this situation the bulk of the low-frequency polarized emission may be concentrated in one half of the galaxy's disk. The strongest effect, demonstrated in Fig. 10, was obtained for a dynamo field possessing an extended magnetic halo, similar to that used in Fig. 9, but a relatively weaker azimuthal field. Such asymmetry is really present in the edge-on galaxies NGC 891 (Hummel et al. (1991) and NGC 4565 (Sukumar & Allen 1991). In NGC 891 the effect has a sense opposite to that expected from the increased field randomness in regions

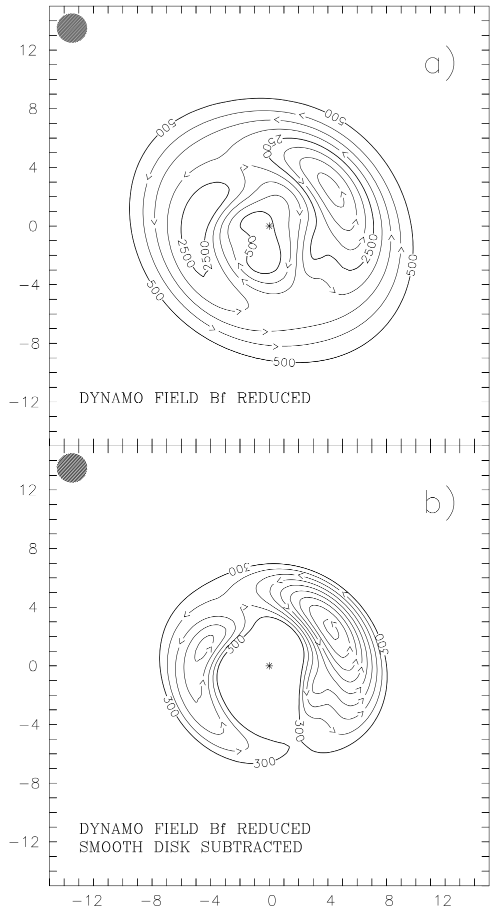


**Fig. 9a and b.** The distribution of low-frequency polarized brightness for a dynamo model possessing an extended magnetic halo with a toroidal component numerically reduced by a factor of 3. **a** the computed polarization model, **b** the same model after subtraction of a disk of uniform brightness

of greater star-forming activity, as a higher polarization is observed in the more intensively star-forming northern half of the disk. We also note that for edge-on galaxies, because of a much longer geometrical pathlength through the disk, Faraday effects may become important at frequencies considerably higher than in face-on objects (Golla & Hummel 1994).

As discussed in Sect. 3.1, helical magnetic tubes larger than the vertical CR-electron scale height show in synchrotron emission only their parts closest to the disk, containing magnetic lines at a certain inclination to the azimuthal direction. In edge-on disks this gives rise to projection effects causing a specific distribution of field components parallel and perpendicular to the line of sight, $B_\|$ and $B_\perp$. In one half of the disk the strongest $B_\|$ (responsible for Faraday rotation) occurs in the disk part closer to the observer than that with highest $B_\perp$ where the bulk of synchrotron emission originates. In such a case strong Faraday rotation is expected. On the other disk side the region of strongest $B_\perp$ lies in the front of that with maximum $B_\|$ which implies much weaker Faraday effects. This asymmetry may lead

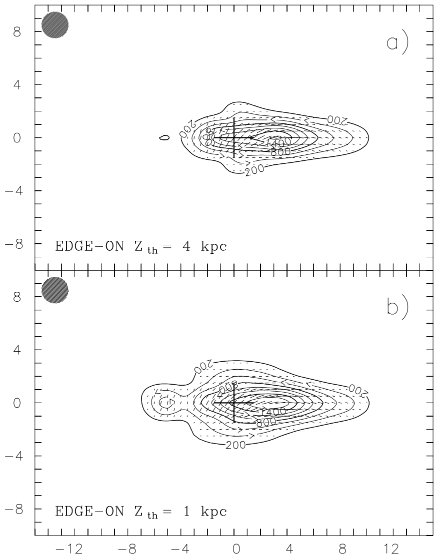


**Fig. 10a and b.** The model distributions of low-frequency polarized emission from edge-on galaxies for the dynamo model with an extended magnetic halo similar to that used in Fig. 9. Two different values of the gaseous disk thickness, 4 kpc and 1 kpc, are used. The cross marks the disk centre

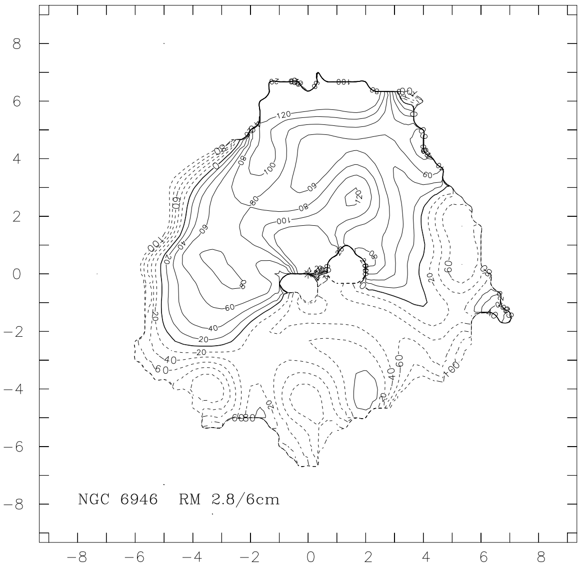


**Fig. 11.** The distribution of the high-frequency ("Faraday-thin" domain) rotation measures in the disk of NGC 6946 as obtained by Ehle & Beck (1993). Solid and dashed contours denote positive and negative values, respectively

also to a much higher depolarization on one side of the disk of edge-on spirals, as demonstrated in Fig. 10.

While in edge-on disks a strong asymmetry occurs for a wide variety of helical fields with tube sizes larger than the CR-electron scale height, in nearly face-on galaxies the effect may be obscured by an interplay of all field components including $B_z$. This yields a much more complex low-frequency polarization picture, dependent on details of distribution of particular field components and of thermal gas, as well as on the degree of beam smearing. While various kinds of asymmetries were obtained for a broad class of field structures, a picture similar to the observed polarization distributions (Fig. 8a) required special adjustments of the magnetic field structure and gas distribution.

### *3.3. Faraday rotation measures*

NGC 6946 belongs to the objects with the best studied distribution of Faraday rotation over its disk (Ehle & Beck 1993). This is due to the fact that the rotation measures were obtained from combining the data at relatively nearby frequencies of 4.85 and 10.57 GHz, both in the high-frequency domain. This allows to avoid the ambiguity in case of rotation of B vectors by more than $90^o$. The map of rotation measures of Ehle & Beck (1993) is shown in Fig. 11.

The map shows a characteristic asymmetry: the region of negative $RM$'s seems to surround that of positive ones. The effect can be qualitatively modeled by an analytically approximated field with an extended magnetic halo (Fig. 12a). The requirement of a very thin layer of toroidal field is much less stringent in this case than was needed to reproduce the polarized arcs. To obtain a strong asymmetry, as shown in Fig. 12a, a gaseous halo with a scale height of 6 kpc was assumed. A hot ($10^6$K), diffuse gas, possessing the tendency to form extended envelopes is known to be quite abundant in nearby galaxies (Ehle et al. 1997a, Schlegel 1994), though the latter author did not yet find clear evidence for an extended hot gaseous corona in NGC 6946. The asymmetry is much weaker for a 2 kpc magnetic disk and a gas scale height of 1 kpc (Fig. 12b).

A strong poloidal field extending high into the halo must contain (by the flux conservation principle) a substantial vertical component which in case of a large gaseous envelope contributes significantly to the Faraday rotation distribution in nearly face-on galaxies. The strongest contribution comes from the part of the halo closer to the observer than the radio bright disk plane. For an assumed sense of the field helicity this "foreground" poloidal field introduces negative rotation measures around the whole outer disk edge and an excess of positive values in the central region. For an inclined galaxy the Faraday effects in the disk halves above and below the major axis occur in different regions of the poloidal field having different local fields strengths and lying at different heights above the disk plane. This makes the maximum excess of positive $RM$ shifted from the centre. All these effects superimposed onto a symmetric $RM$ distribution caused by a toroidal field may give rise to the asymmetry shown in Fig. 12a.

All the models considered yielded a non-zero mean Faraday rotation emulating some contribution to the foreground rotation. This is due to the fact that the condition div $B = 0$ implies a much stronger vertical field and Faraday rotation in the disk centre than in its outer regions. As most of $RM$ originates in the halo part in front of the disk plane this gives rise to a non-zero

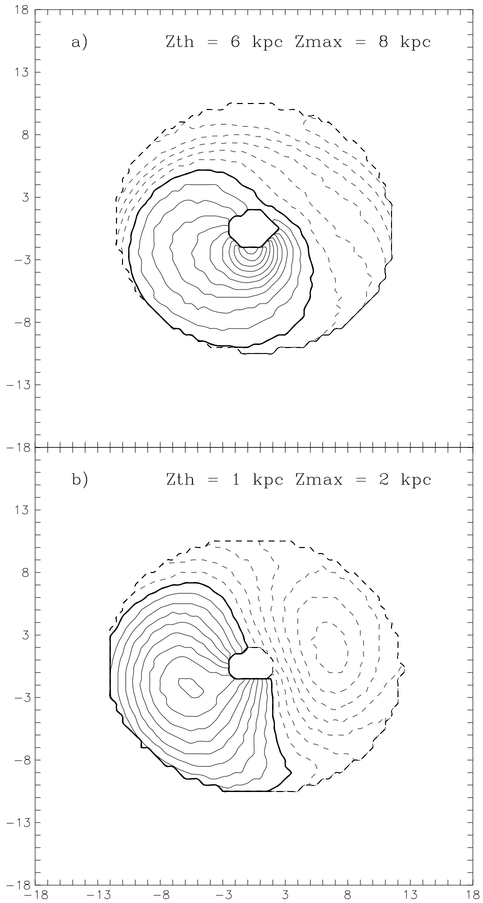


**Fig. 12a and b.** Distributions of high-frequency Faraday rotation measures for analytical field models: **a** for a large magnetic halo extending up to 8 kpc (shown in Fig. 2), accompanied by a gaseous halo of vertical scale height 6 kpc, and **b** for a magnetic disk of thickness 2 kpc and a vertical gas scale height of 1 kpc (**b**). Solid and dashed contours denote positive and negative values, respectively. The contour step corresponds to a Faraday rotation angle of $5^o$

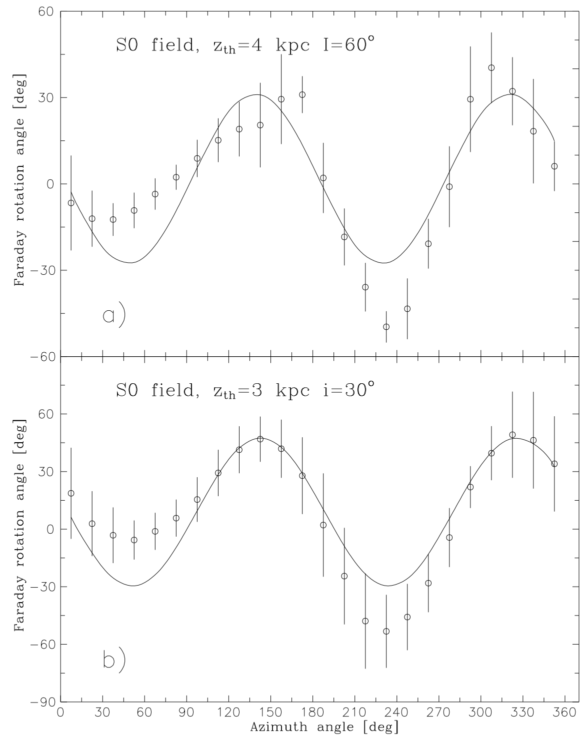


**Fig. 13a and b.** The azimuthal variations of high-frequency ("Faraday-thin" domain) rotation measures for a magnetic field computed from the dynamo theory with a weak diffusion in the halo, the same as used to model the polarization of edge-on disks (Fig. 10). A near edge-on (a) and near face-on (b) case is considered. The vertical bars show the pixel-to-pixel scatter of $RM$ in the model maps, solid curves present the fit of doubly-periodic sine functions with adjustable amplitude, period and phase

net rotation measure averaged over the whole disk. The models shown in Fig. 12a, b were corrected for this "foreground" component corresponding to $RM$ of about 20 rad/m$^2$, determined from the azimuthal $RM$ distribution in the model map in the same way as was done already for NGC 6946 (Fig. 11) by Ehle & Beck (1993).

Simple, analytical fields usually give singly-periodic variations of Faraday rotation with azimuthal angle in the disk, characteristic for classical axisymmetric structures. Nevertheless, one dynamo-computed field with weak turbulent diffusion in the halo (used to model edge-on galaxies, Sect. 3.2), possessing an extended magnetic envelope and a strong reversed toroidal field at large heights (like that discussed in M51 by Berkhuijsen et al. 1996), produced the impression of a bisymmetric field (Fig. 13a and b). The effect is present in the "Faraday-thin", high-frequency domain, though for galaxies with low ionized gas densities (e.g. M81) it may remain visible at frequencies much lower than 5 GHz. It depends only weakly on the galaxy inclination and may occur in both nearly face-on and nearly edge-on objects. The effect may result from a complex interplay of Faraday rotations in the disk plane and high in the halo, yielding a combination of two singly-periodic azimuthal changes of $RM$ shifted in phase by $180^o$, because of an opposite sign of $B_r$ and $B_\phi$ in these regions. Thus, the necessary condition to obtain the BSS-type azimuthal $RM$ variations is the existence of a thick layer of toroidal field reversing at 2-3 kpc above the disk plane in addition to an extended, dilute gaseous corona and the poloidal field penetrating highly into the halo. However, other dynamo models studied, having also a strong, reversed toroidal field in the halo do not show clear signs of a BSS-type curve. Thus, other details of magnetic field structure are important, too.

The application of this result to real galaxies is somewhat complicated. M81, the only object with a clear BSS-type variation of rotation measures (Krause et al. 1989), is weakly forming stars and probably does not possess any extended gaseous halo; it also shows highly non-axisymmetric kinematics. Attempts to involve the effect in explaining the deviations of azimuthal variations of $RM$ from the singly-periodic behaviour in M83

(Ehle et al. 1997b) would require a magnetic field model (strong azimuthal halo field) different from that needed to best reproduce the low-frequency polarization image (a thin disk of azimuthal field). In M51 where Berkhuijsen et al. (1996) present more direct evidence for the reversed halo field, the variations of $RM$ over the disk are too complex for any definite conclusions. Despite these complications the model demonstrates that the apparent signatures of a BSS-type field can occur for an axisymmetric magnetic field as well. We note finally that when Faraday rotation angles approach $90^o$ the azimuthal $RM$ variations in all models start to show one or more sudden jumps, constituting signatures of a "Faraday-thick" regime.

## 4. Discussion

In this paper we attempted to reproduce a number of polarization properties of spiral galaxies assuming a quadrupole-type axisymmetric helical field, easiest to excite in dynamo models, and naturally expected from interstellar processes like turbulence and diffusion. Models with *magnetic tubes twisted on relatively small scales* seem to be ruled out by the existing data on the cosmic-ray vertical scale heights, though they may be still applicable for galaxies similar to M31, i.e. dominated by a single radio emitting ring or torus running around the disk, and possessing a relatively small CR scale height. In principle, the model could be still improved by assuming e.g. tubes with dimensions $< 1$ kpc in the disk plane, but stretched vertically up to several kiloparsecs. Such a possibility, though physically possible has no other observational support and has not been further considered.

Effects like the arc-like distribution of the low-frequency polarized intensity and the specific asymmetries of high-frequency Faraday rotation are found to be typical signatures of *axisymmetric large-scale helical fields*, possessing radial and vertical components twisted over scales of several kiloparsecs. However, reproduction of asymmetric arcs and BSS-type distributions of the high-frequency rotation measure by axisymmetric fields needs their two different models. The first effect observed in M83 needs a strong poloidal field in the halo with a toroidal field confined to a very thin layer in the disk plane. On the other hand, an explanation of the observed (not singly-periodic) azimuthal changes of $RM$ in the same galaxy by doubly-periodic variations produced in an axisymmetric helical field (Fig. 13a and b) requires a strong toroidal field extending up to several kpc into the halo. A third possibility also exists: the dynamo field used to construct the BSS-type curve shown in Fig. 13a and b also yields some extremely weak signs of low-frequency arcs, which can be enhanced by opacity effects (cf. Sect. 3.2). However, a more detailed study requires the introduction of effects like Faraday dispersion into our model and will be a subject of future studies. We also found that the existing dynamo fields need substantial modifications to reproduce the observational data.

We note that the two kinds of magnetic field models mentioned imply different conditions in the galactic halo. In the $\alpha\Omega$-dynamo model the poloidal field is produced from a toroidal one by helical turbulent motions (called $\alpha$-effect), while the latter component is reconstructed from the poloidal field by a differential rotation ($\Omega$-effect). To reproduce the asymmetric rings we need both processes of comparable importance in a thin disk, and the halo dominated by the $\alpha$-effect. In contrast to that, an impression of a BSS-field is obtained if the $\alpha$-and $\Omega$-effects are of comparable strength in disk and halo. The kinematics of the gas in the galactic halo is poorly known. We note, however, that recent HI observations of NGC 891 suggest the rotational velocity decreasing with distance from the disk plane (Swaters et al. 1996). Further observational studies of the gas kinematics high in the galactic halo are of great importance for future progress of the dynamo theory and for understanding the polarization properties of spiral galaxies.

The vertical magnetic field component present in our large-scale models does not imply strong signatures of vertical fields in edge-on disks. In the case of an extended magnetic halo the vertical component dominates at much higher z than the CR-electron scale height. For a thin magnetic disk $B_z$ becomes much smaller than $B_r$ and $B_\phi$. Both cases yield the observational picture of a magnetic field generally parallel to the disk plane.

Our large-scale magnetic field models still need a small-scale component to lower the expected polarization degree to values observed in real galaxies either by geometrical depolarization or by its contribution to the Faraday dispersion. The formation of large-scale fields from smaller helical structures does not necessarily mean that the latter do not exist at all. We can rather expect a hierarchical cascade of helical twisting and tube-like features from the galactic scale down to a few tens of parsecs. In this picture, the helical field twisting at scales larger than CR vertical scale heights would be responsible for observed asymmetries. The structures twisted at scales smaller than those of the CR distribution would contribute little to the global asymmetries (Sect. 3.1), acting as random fields lowering the overall polarization degree (cf. Otmianowska-Mazur et al. 1992) and introducing the opacity effects due to Faraday dispersion.

Possible azimuthal variations of the uniform field strength (e.g. the magnetic arms detected in NGC 6946 by Beck & Hoernes 1996) may cause azimuthal modulations in the high-frequency polarization distribution, rather weak if observed with a modest resolution. No strong influence on the distribution of Faraday rotation (arising in our models mostly in an extended halo) is expected if the variations were due to field tangling by star-forming processes, most efficient in a thin (100 pc) disk. The effect on the low-frequency polarized arcs which in our models results from an interplay of polarized emission from a 1 kpc thick CR-electron disk and Faraday rotation assumed to occur up to several kpc in the halo is unknown. We expect that at low resolution the effect would be largely smeared out by a large beam, though a more detailed model is needed. Moreover, we could best reproduce the ring-like structure for M83, which has a much smaller arm/interarm star formation contrast than NGC 6946.

In many cases our models qualitatively reproduced some characteristics of the polarization and Faraday rotation structure, while significant details still differ (cf. Figs 11 and 12 a-b). This fact mostly follows from the very simple forms of the field geometry as well as of the CR and thermal gas distributions adopted. An admixture of non-axisymmetric components is also probable. To achieve further progress, we state an urgent need for further observational and theoretical efforts in both dynamo theory and polarization/Faraday rotation studies of spiral galaxies.

## 5. Summary and conclusions

The axisymmetric helical magnetic field structures expected from dynamo models and from turbulent and diffusive processes in the interstellar medium were used to reproduce some polarization properties of spiral galaxies. Both possibilities, the galactic disk filled with small-scale magnetic tubes or global dynamo-type fields, were considered. In the latter case we used either analytical approximations or computational results from dynamo models. The following results were obtained:

- A coherent spiral pattern of polarization B-vectors can be reproduced by both small- and global-scale helical axisymmetric fields. However, small-scale ($< 1$ kpc) helical fields poorly reproduce the observed pitch angle distribution of polarization B vectors if realistic CR electron vertical scale heights are adopted. Large-scale fields also reproduce the azimuthal variations of the observed pitch angles of B vectors.
- Large-scale axisymmetric helical fields qualitatively reproduce many observed facts thought to signify non-axisymmetric phenomena, like the arc-like distributions of the low-frequency polarized emission in moderately inclined spirals, asymmetric distributions of polarized brightness in edge-on galaxies, specific high-frequency $RM$ asymmetries or doubly-periodic variations of the rotation measure with azimuthal angle in the disk.
- The assumption of an extended (several kpc) gaseous and magnetic halo provides a reasonable fit to the data.
- To reproduce the data properly, the azimuthal field cannot be much stronger than the poloidal one.
- The best reproduction of the asymmetries of low-frequency polarized intensity and of Faraday rotation was obtained for azimuthal fields having a much smaller vertical extent than the poloidal one. This implies a strong increase of an intrinsic field pitch angle from the disk to the halo.
- Bisymmetric-like variations of the high-frequency rotation measure and the low-frequency polarization arcs need two different kinds of axisymmetric fields: with and without strong toroidal fields high above the disk plane. Their occurrence may depend on the relative importance of helical turbulence and differential rotation in the disk and halo.
- Magnetic fields twisted over scales smaller than 1 kpc (serving as a random field), or other types of small-scale field fluctuations are still needed to explain the low overall polarization observed in galactic disks.

Our results show some directions of future developments of dynamo theory. In particular, the possibility to obtain a thick magnetic halo with strong radial and vertical components and a thin layer of a toroidal one should be investigated. A substantial expansion of the existing observational data on polarization and Faraday rotation in spiral galaxies is required as well.

*Acknowledgements.* The authors are indebted to Professors Richard Wielebinski from the Max-Planck-Institut für Radioastronomie (MPIfR) in Bonn and Günther Rüdiger from the Astrophysical Institut Potsdam (AIP) for their support and valuable discussions during this work. One of us (M.U.) wants to express a particular gratitude to Prof. Wielebinski and to Prof. Karl-Heinz Rädler, Astrophysical Institute in Potsdam, for the invitations to stay at MPIfR and AIP where substantial parts of this work were done. We wish to express our profound gratitude to Dr Elly M. Berkhuijsen from MPIfR for her critical reading of the manuscript and for her valuable comments which greatly improved the scientific content, style and language of this paper. We are particularly grateful to Dr K. Ferrière for her valuable comments on the final version of the paper. The authors are also indebted to Drs. K. Otmianowska-Mazur and M. Ostrowski from the Astronomical Observatory of the Jagiellonian University in Krakow for their valuable comments. This work was supported by a grant from the Polish Research Committee (KBN), grant no. PB. 0628/P3/93/04. Large parts of computations were made using the HP715 workstation at the Astronomical Observatory in Krakow, partly sponsored by the ESO C&EE grant A-01-116, and using the Convex-SPP machine at the Academic Computing Centre "Cyfronet" in Krakow.

## References

Beck R., 1982, A&A 106, 121
Beck R., 1991, A&A 251, 15
Beck R., 1997, in Lesch H. et al., "The Physics of Galactic Halos", Akademie-Verlag, Berlin, p. 135
Beck R., Brandenburg A., Moss D., Shukurov A., Sokoloff D., 1996, Ann. Rev. A&A 34, 155
Beck R., Hoernes P., 1996, Nature 379, 47
Berkhuijsen E.M., Horellou C., Krause M., Neininger N., Poezd A.D., Shukurov A., Sokoloff D.D, 1996, A&A, in press
Chiba M., 1993, in Krause F., Rädler K.-H., Rüdiger G. (eds.) Proc. IAU Symp. 157, The Cosmic Dynamo, Kluwer, Dordrecht p.373
Donner K.J., and Brandenburg A., 1990, A&A 240, 289
Dumke M., Krause M., Wielebinski R., Klein U., 1995, A&A 302, 691
Ehle M., Beck R., 1993, A&A 273, 45
Ehle M., Pietsch W., Beck R., Klein U., 1997a, A&A, submitted
Ehle M., Beck R., Haynes R.F., Sukumar S., 1997b, MNRAS, submitted
Elstner D., Meinel R., Beck R., 1992, A&A Suppl. 94, 587
Golla G., Hummel E., 1994, A&A 284, 777
Horellou C., Beck R., Berkhuijsen E.M., Krause M., Klein U., 1992, A&A 265, 417
Hummel E, Beck R., Dahlem M., 1991, A&A 248, 23
Krause, M., Beck R., Hummel E., 1989, A&A 217, 17
Lesch H., 1993, in Krause F., Rädler K.-H., Rüdiger G. (eds.) Proc. IAU Symp. 157, The Cosmic Dynamo, Kluwer, Dordrecht p. 395
Neininger N., Beck R., Sukumar S., Allen R.J., 1993, A&A 274, 687
Otmianowska-Mazur K., Urbanik M., Terech, A., 1992, Geophys Astrophys. Fluid. Dyn. 66, 209
Otmianowska-Mazur K., Urbanik M., 1994, Geophys Astrophys. Fluid. Dyn. 75, 61
Pacholczyk A.G., 1979, "Radio Astrophysics", Freeman, S. Francisco
Pouquet, A., Frisch, U., Leorat, J., 1976, J. Fluid Mech. 77, 321

Schlegel E.M., 1994, ApJ 434, 523
Segalovitz A., Shane W.W., de Bruyn A.G., 1976, Nature 264, 222
Soida M., Urbanik M., Beck R., 1996, A&A 312, 409
Sukumar S., Allen R.J., 1989, Nature 340, 537
Sukumar S., Allen R.J, 1991, ApJ 382, 100
Swaters R.A., Sancisi R., van der Hulst J.M., 1996 in Bender R., Davies R.L. (eds.) Proc. IAU Symp 171, New Light on Galaxy Evolution, Kluwer, Dordrecht p. 450
Urbanik M., Otmianowska-Mazur K., 1993 in Krause F., Rädler K.-H., Rüdiger G. (eds.) Proc. IAU Symp. 157, The Cosmic Dynamo, Kluwer, Dordrecht p. 411
Urbanik M., Otmianowska-Mazur K., Beck R., 1994, A&A 287, 410
Wielebinski R., Krause F., 1993 A&A Rev. 4, 691

This article was processed by the author using Springer-Verlag LaTeX A&A style file *L-AA* version 3.